



HAL
open science

Infrared thermography of fatigue in metals

Minh-Phong Luong

► **To cite this version:**

Minh-Phong Luong. Infrared thermography of fatigue in metals. Thermosense XIV: An Intl Conf on Thermal Sensing and Imaging Diagnostic Applications, Apr 1992, Orlando, United States. pp.222-233, 10.1117/12.58539 . hal-04667426

HAL Id: hal-04667426

<https://hal.science/hal-04667426v1>

Submitted on 3 Sep 2024

HAL is a multi-disciplinary open access archive for the deposit and dissemination of scientific research documents, whether they are published or not. The documents may come from teaching and research institutions in France or abroad, or from public or private research centers.

L'archive ouverte pluridisciplinaire **HAL**, est destinée au dépôt et à la diffusion de documents scientifiques de niveau recherche, publiés ou non, émanant des établissements d'enseignement et de recherche français ou étrangers, des laboratoires publics ou privés.



Distributed under a Creative Commons Attribution - NonCommercial 4.0 International License

Infrared thermography of fatigue in metals

Minh Phong Luong

CNRS - LMS, Ecole Polytechnique
91128 Palaiseau - France

ABSTRACT

This paper aims to illustrate the use of infrared thermography as a nondestructive and noncontact technique (a) to observe the physical processes of damage and fatigue on metallic specimens subjected to rotating bending loadings, (b) to detect the occurrence of energy dissipation and (c) to evaluate the limit of endurance of the tested materials.

1. INTRODUCTION

Engineering structures are frequently subjected to cyclically varying loads or deformations and also to some form of multiaxial stressing. In addition, many components have design details which involve severe stress concentrations. At these highly stressed locations, the stress (or strain) on many occasions will exceed well above the conventional elastic limit. Conditions of this type are extremely common and are often the cause of premature failure in pieces of equipment intended for longlife applications. The phenomenon of progressive deterioration of the strength due to the action of repeated load cycles is usually referred to as "fatigue".

In recent years, fracture mechanics has become the primary approach to controlling brittle fracture and fatigue failures in structures. Experimental methods which have been used to obtain the fatigue characteristics of materials, usually correlate the fatigue life of a smooth specimen under uniaxial stress conditions with either plastic strain or stress amplitude. Multiaxial fatigue assessment is then carried out with the help of an appropriate rule or criterion that reduces the complex multiaxial loading to an "equivalent" uniaxial loading. In these approaches, the relationship between the cyclic stress and plastic strain, and the fatigue damage process is usually overlooked²⁰. Since the fatigue damage is generally caused by the cyclic plastic strain, the plastic strain energy plays an important role in the damage process. Fatigue cracks generally initiate from surface defects or discontinuities and are thus predominantly influenced by the surface stress system. The significance of the energy approach is in its ability to unify microscopic and macroscopic testing data, and subsequently to suggest multiaxial design criteria. Therefore, the idea of relating fatigue life to the intrinsic dissipation detected by infrared thermography seems to be highly relevant.

This paper emphasizes the application of infrared thermography to damage and fatigue evaluation of metallic materials, and subsequently to non destructive testing and integrity control on steel structures.

2. FATIGUE ET ENDURANCE OF MATERIALS

When subjected to cyclically varying loads, metals break at stresses that are much lower than the ordinary fracture stress measured under static conditions. This loss of strength under alternating load conditions is called *fatigue*. In typical fatigue behavior the fracture stress (i.e., the peak stress amplitude) decreases with the number of load reversals according to a curve whose general shape is the Wöhler curve, an S-N (stress vs. number of cycles) or *endurance* curve. In cyclic loading, a material can safely support a given peak stress amplitude for only a specified number of cycles, given by the endurance curve, before it breaks. In some cases, the endurance curve may level off for a limiting stress amplitude called the *fatigue endurance limit*, below which the solid can support the load indefinitely without danger of fracture.

The most common method of obtaining fatigue endurance data is the rotating-beam test. The rotating specimen is loaded in bending so that the peak-stress alternations are experienced only at the outer edge of the cross-section.

The local nature of the phenomenon of fatigue failure makes it necessary to trace carefully the path which the applied loads take within the structure, because a fatigue crack can start in one small region of high alternating stress and can lead to complete failure even though the rest of the structure is very strong. The loads must be traced through the structure to the subcomponents, and the stress distribution within the subcomponent must be analyzed to find the critical regions of high stress.

The plastic strain energy per cycle ΔW is the area of the hysteresis loop and the total plastic strain energy $W_f = \Sigma \Delta W$. The phenomenon of the fatigue damage is primarily controlled by the stress and plastic strain or the irrecoverable plastic strain energy per cycle⁸. Each material has a capacity to absorb a certain amount of energy and when this limit is attained, "fatigue failure" results. The fatigue failure is sometimes defined in terms of a crack length for the load-controlled tests, and a drop in the peak stress for the strain-controlled tests.

In total strain-controlled experiments, it has been observed that the plastic strain energy per cycle ΔW does not vary appreciably with cycles. However, when a specimen is subjected to cyclic loading with fully reversed loads, the strain varies depending upon the pretest history of the material. Thus the plastic strain energy per cycle will also vary during the life. For a material which cyclically softens, the plastic strain and the corresponding energy per cycle will increase, whereas for the hardening material they will decrease. During the transient state when hardening or softening occurs, the plastic strain energy and mean value of strain per cycle may change considerably, before an apparent steady state is achieved.

3. HEAT PRODUCTION MECHANISM DURING FATIGUE PROCESS

Fatigue cracks in individual crystals are generally assumed¹² to develop within glide bands. The reason for the start of a fatigue crack is the embrittlement of the material within the glide bands due to gradual exhaustion, under reversed stressing, of potential slip planes. A more specific mechanism⁹ of fatigue-crack-initiation within glide bands is the development of highly generated temperature and associated thermal stress-gradients in the fronts of any active slip plane, resulting from the conversion into heat of the work in slip of the applied forces. The concept of temperature-flash³ accounting for crack initiation under repeated stressing provides a plausible explanation for the observed thermal softening in fatigue of previously cold-worked metal. This is consistent with the assumption that under repeated stressing, relatively high temperatures are developed within the glide bands. The distribution and the character of glide bands under conditions of relatively rapidly applied repeated stress-cycles differ significantly from that produced by unidirectional stressing.

The localization of slip under rapidly applied repeated stress cycles are explained by the consideration of the transiently viscous response of newly formed slip-bands²⁹ which appear to be the result of transient disorder within the slipped region. Shear stresses in such bands are relieved almost immediately after their formation. Slip under partly or totally reversed rapidly applied repeated stress cycles is thus sharply concentrated within the regions of initial slip by the same process of quasi-viscous stress relaxation along newly formed slip-band that causes outward spreading of slip in unidirectional stressing. The local temperature increase, on individual slip planes or within a cluster of slip planes, is high enough to produce, in the vicinity of the slip region, localized thermal stresses of the order of magnitude of the tensile strength of the metal. The development of localized high temperatures, in the course of sharply localized slip, might be considered a plausible mechanism of fatigue crack initiation.

The question of when does a crack "initiate" to become a "propagating" crack, seems to be somewhat philosophical. This paper aims to introduce the infrared thermographic technique which can quantitatively evaluate the occurrence of both initiation and propagation, establish allowable stress levels and inspection requirements so that fractures cannot occur. In addition, this technique describes the failure location and process of the structure failure.

Infrared thermography has been successfully used as an experimental method for detection of plastic deformation during crack propagation of a steel plate under monotonic loading⁴ or as a laboratory technique for investigating damage, fatigue and creep mechanisms occurring in engineering materials²⁴.

This experimental tool is used to detect the onset of unstable crack propagation and/or flaw coalescence due to the thermomechanical coupling, when increasing irreversible microcracking is induced by vibratory loading.

3.1. Coupled thermo-visco-elastic-plastic analysis

Traditionally, thermomechanical coupling effects have been neglected in thermal analyses. It is generally assumed that the inelastic deformation is rate(time)-independent at low homologous temperatures. The theory of plasticity is consequently formulated in a rate(time)-independent fashion and phenomena such as loading rate sensitivity, creep and relaxation are excluded. The temperature field and the deformation induced by thermal dilation and mechanical loads were solved separately. However this effect could become noticeable if the material is significantly loaded beyond its reversible threshold.

The development of the thermo-visco-elastic-plasticity equations requires three types of basic assumptions²⁻⁷⁻¹³⁻¹⁴⁻²⁶ :

- a) The basic thermomechanical quantities describing thermodynamic processes : the motion x , the second Piola-Kirchhoff stress tensor S , the body force per unit mass b , the Helmholtz free energy ψ , the specific entropy s , the heat supply r_0 , the absolute temperature T , the heat flux vector per unit area q , the inelastic strain tensor E^I and a set of internal state variables $\alpha^{(I)}$ characterizing the material.
- b) The fundamental equations of mechanics postulating for the balance laws of linear momentum, angular momentum, and energy, as well as the second law of thermodynamics expressed in the variables given in a) :

- (i) balance of linear momentum

$$\nabla S F^T + \rho (b - \ddot{x}) = 0 \quad (1)$$

where F denotes the transformation gradient.

- (ii) conservation of energy

$$\rho (\dot{\psi} + \dot{s}T + s\dot{T}) = \rho \dot{e} = S : \dot{E} - \text{div } q + r_0 \quad (2)$$

- (iii) second law of thermodynamics

$$- \rho (\dot{\psi} + s\dot{T}) + S : \dot{E} - q \cdot (\nabla T)/T \geq 0 \quad (3)$$

where ρ (kg m^{-3}) is the mass density in the reference configuration,
 e the specific internal energy and
 E the Green-Lagrange strain tensor $E = (\nabla x^T \cdot \nabla x - 1)/2$.

The superposed dot stands for the material time derivative. The continuity equation and the balance of angular momentum are implicitly satisfied in the fundamental equations.

- c) The constitutive assumptions describing the material response and abiding the compatibility of the constitutive equations with the fundamental equations of mechanics.
When adopting the separability of the strain tensor

$$E = E^e + E^I + \beta (T - T_R) \quad (4)$$

where β is the coefficient of the thermal expansion matrix and T_R the reference temperature, the requirement of inequality (4) yields :

- (i) The response functions S , ψ and s are independent of the temperature gradient ∇T .
- (ii) ψ determines both the stress tensor and the specific entropy through

$$S = \rho \partial\psi/\partial E^e \quad \text{and} \quad s = -\partial\psi/\partial T + (\partial\psi/\partial E^e) : \beta$$

(iii) ψ , \dot{E}^I and q obey the general inequality

$$(S - \rho \partial\psi/\partial E^I) : \dot{E}^I - q \cdot \nabla T/T \geq 0 \quad (5)$$

The above thermodynamic restrictions may now be applied to equation (2) yielding :

$$\begin{aligned} \rho (\partial\psi/\partial E^I - T \partial^2\psi/\partial T \partial E^I) : \dot{E}^I - T(\partial S/\partial T) : \dot{E}^e - \rho T(\partial^2\psi/\partial T^2)\dot{T} + \dot{S} : \beta T \\ = S : \dot{E}^I - \text{div } q + r_0 \end{aligned} \quad (6)$$

Assuming

$$\psi = \psi_0 + (E^e : \overset{4}{D} : E^e)/2 - C_v T \ln (T/T_R - 1) \quad (7)$$

and the Fourier heat conduction law

$$q = -K \text{ grad } T \quad (8)$$

where ψ_0 , $\overset{4}{D}$, C_v and K are material constants. $\overset{4}{D}$ stands for the fourth-order elasticity tensor.

C_v (J kg⁻¹ K⁻¹ : Joule per kilogramme per Kelvin degree) is the specific heat at constant deformation and K (W m⁻¹ K⁻¹ : Watt per metre per Kelvin degree) is the thermal conductivity.

Finally we get the coupled thermomechanical equation :

$$\rho C_v \dot{T} = K \nabla^2 T - (\beta : \overset{4}{D} : \dot{E}^e) + S : \dot{E}^I + r_0 \quad (9)$$

which shows the varied potential applications and uses of the infrared scanning technique in engineering problems.

The volumetric heat capacity $C = \rho C_v$ of the material is the energy required to raise the temperature of an unit volume by 1 °C (or Kelvin degree).

3.2. Thermal conduction

The first term on the right hand side of the thermomechanical equation governs the transference of heat by thermal conduction in which the heat passes through the material to make the temperature uniform in the specimen.

The second-order tensorial nature of the thermal conductivity K may sometimes be used for the detection of anisotropy of heavily loaded materials.

Where an unsteady state exists, the thermal behaviour is governed not only by its thermal conductivity but also by its heat capacity. The ratio of these two properties is termed the thermal diffusivity $\alpha = K/C$ (m² s⁻¹) which becomes the governing parameter in such a state. A high value of the thermal diffusivity implies a capability for rapid and considerable changes in temperature.

It is important to bear in mind that two materials may have very dissimilar thermal conductivities but, at the same time, they may have very similar diffusivities.

3.3. Thermoelasticity

The second term illustrates the thermoelastic effect. Within the elastic range and when subjected to tensile or compressive stresses, a material experiences a reversible conversion between mechanical and thermal energy causing it to change temperature.

Provided adiabatic conditions are maintained, the relationship between the change in the sum of the principal stresses and the corresponding change in temperature is linear and independent of loading frequency. It is the reversible portion of the mechanical energy generated ; this thermoelastic coupling term may be significant in cases of isentropic loading.

3.4. Intrinsic dissipation

The third term is the energy dissipation generated by viscosity and/or plasticity. Internal energy dissipation was recognized by many scientists. The work done to the system by plastic deformation is identified as the major contribution to the heat effect.

In thermo-elastic-plasticity, there exists a general acceptance that not all the mechanical work produced by the plastic deformation can be converted to the thermal energy in the solid. A larger portion of the work is believed to have been spent in the change of material microscopic structure as shown in Table I.

The work done in plastic deformation per unit volume can be evaluated by integrating the material stress/strain curve.

This internal dissipation term constitutes an important part of the nonlinear coupled thermomechanical effect.

\mathcal{FV} = Internal variables and postulations	Stored energy at microlevel	Internal energy dissipation rate	Heat to plasticity
Dillon ⁷ : No \mathcal{FV} ϵ_{ij}^P responsible for D	0	$\sigma_{ij} \dot{\epsilon}_{ij}^P = \sigma'_{ij} \dot{\epsilon}'_{ij}^P$	0
Lee ¹⁵ : \mathcal{FV} = plastic power $\sigma_{ij} \dot{\epsilon}_{ij}^P$	$(1-\gamma) \sigma_{ij} \dot{\epsilon}_{ij}^P$ $0.9 \leq \gamma \leq 1.0$	$\gamma \sigma_{ij} \dot{\epsilon}_{ij}^P$	0
Nied-Batterman ²² : $\chi \dot{\omega} = \sigma_{ij} \dot{\epsilon}_{ij}^P$ with $\mathcal{FV} = \omega$ χ = dislocation energy	$\Lambda \sigma_{ij} \dot{\epsilon}_{ij}^P$ Λ = energy stored/inelastic energy expanded	$(1-\Lambda) \sigma_{ij} \dot{\epsilon}_{ij}^P$	$T\chi \frac{\partial \Lambda}{\partial \chi}$
Raniecki-Sawczuk ²³ : \mathcal{FV} = work-hardening K $K = \omega(\sigma_{ij}, T) \sigma_{ij} \dot{\epsilon}_{ij}^P$ ω = integrating factor	$\chi(K, T) \dot{K}$	$\sigma_{ij} \dot{\epsilon}_{ij}^P - \pi \dot{K}$ $\pi = \mathcal{FV}$ conjugate	$T \frac{\partial \pi}{\partial T}$
Mroz-Raniecki ²¹ : $\mathcal{FV} = K$ $\dot{K} = \sigma_{ij} \dot{\epsilon}_{ij}^P - \pi \dot{K}$ $\pi = -\frac{\partial D}{\partial K}$	$\sigma_{ij} \dot{\epsilon}_{ij}^P - \pi \dot{K}$ $\pi = -\frac{\partial D}{\partial K}$	$\sigma_{ij} \dot{\epsilon}_{ij}^P - \pi \dot{K}$	$T \frac{\partial \pi}{\partial T} = 0$
Lehman ¹⁶ : $\mathcal{FV} = K$ $K = (1-\xi) \sigma_{ij} \dot{\epsilon}_{ij}^P$ ξ = experimentally determined constant	$\dot{K} = (1-\xi) \sigma_{ij} \dot{\epsilon}_{ij}^P$	$\xi \sigma_{ij} \dot{\epsilon}_{ij}^P$	0

Table I - Thermo-elastic-plastic couplings

The quantification of this intrinsic dissipation for engineering materials is an extremely difficult task if infrared thermography is not used. This chapter emphasizes the advantages of the infrared thermographic technique for the detection of this thermomechanical effect.

3.5. Heat sources

The last term shows the existence of sources or sinks of heat in the scanning field. The surface heat patterns displayed on the scanned specimen may be established either by external heating referred to in literature²⁴ as "passive heating" where local differences in thermal conductivity cause variations on isothermal patterns or by internally generated heat referred to as "active heating" where isothermal patterns are established by the transformation of internal energy into heat.

In the case of forced convection, if fluid at the temperature of the medium is forced rapidly past the surface of the solid, it is found experimentally that the rate of loss of heat from the surface is proportional to the surface conductance or coefficient of surface heat transfer. This fact has been used for the detection and location of heat, gas or fluid leakage through rock-like materials.

4. INFRARED THERMOGRAPHIC EVALUATION OF ENDURANCE LIMIT

Infrared thermography has been successfully used as an experimental method for the detection of plastic deformation during crack propagation of a steel plate under monotonic loading⁴ or as a laboratory technique for investigating damage, fatigue and creep mechanisms occurring in engineering materials¹⁷⁻¹⁸⁻¹⁹⁻²⁴.

This experimental tool is used to detect the stress concentration, the onset of unstable crack propagation and/or flaw coalescence due to the thermomechanical coupling, when increasing irreversible microcracking is induced by vibratory loading.

4.1. Infrared thermography

Infrared thermography is a technique for producing heat pictures from the invisible radiant energy emitted from stationary or moving objects at any distance and without surface contact or in any way influencing the actual surface temperature of the objects viewed.

A scanning camera is used which is analogous to a television camera. It utilizes a infrared detector in a sophisticated electronics system in order to detect radiated energy and to convert it into a detailed real time thermal picture in a video system both color and monochromatic. Response times are shorter than a microsecond. Temperature differences in heat patterns as fine as 0.1 °C are discernible instantly and represented by several distinct hues.

This technique is sensitive, nondestructive and noncontact, thus suited for records and observations in real time of heat patterns appearing on the surface of an object being scanned. No interaction at all with the specimen is required to monitor the thermal gradient.

The quantity of energy W ($W\ m^{-2}\ \mu m^{-1}$) emitted as infrared radiation is a function of the temperature and emissivity of the specimen. The higher the temperature, the more important is the emitted energy. Differences of radiated energy correspond to differences of temperature.

4.2. Infrared Scanner

As an example, the AGA 782 SW infrared scanner unit¹ comprises :

- a) a set of infrared lens which focusses the electromagnetic energy radiating from the object being scanned into the vertical prism,
- b) an electro-optical scanning mechanism which discriminates the field of view in 10 000 pixels by means of two rotating vertical (180 rpm) and horizontal (18 000 rpm) prisms with a scanning rate of 25 fields per second,
- c) a set of relay optics containing a selectable aperture unit and a filter cassette unit which focusses the output from the horizontal prism onto a single element point detector, located in the wall of a Dewar chamber,
- d) a photovoltaic SW short waves infrared detector composed of Indium Antimonide InSb which produces an electronic signal output varying in proportion to the radiation from the object within the spectral response 3.5 μm to 5.6 μm ,

- e) a liquid nitrogen Dewar which maintains the InSb detector at a temperature of $-196\text{ }^{\circ}\text{C}$ allowing a very short response time of about one microsecond,
- f) and a control electronics with preamplifier which produces a video signal on the display screen.

Since the received radiation has nonlinear relationship to the object temperature, and can be affected by atmosphere damping and includes reflected radiation from object surroundings, calibration and correction procedures have to be applied. Knowing the temperature of the reference, the object temperature can then be calculated with a sensitivity of $0.1\text{ }^{\circ}\text{C}$ at $30\text{ }^{\circ}\text{C}$.

4.3. Rotating bending tests

The material for the rotating bending tests was a XC55 steel, quite extensively used in automobile construction. To minimize scatter, the 6.74 mm in diameter specimens have been prepared from a single melt. The number of load cycles was 10^7 corresponding to the automobile fatigue damage. Cyclic fatigue tests were performed on a 4-point loading rotating bending Schenck machine (Fig. 1) running at approximately 100 Hz . A total of 18 specimens was step-tested, meaning that each specimen was run for 10^7 cycles at 370 MPa , whereupon the stress was raised in 10 MPa step if there is nonfailure and the stress is lowered in case of failure. Using standard methods of statistical analysis, the fatigue limit has been estimated equal to 399 MPa with a standard deviation of 41 MPa (Fig. 2).

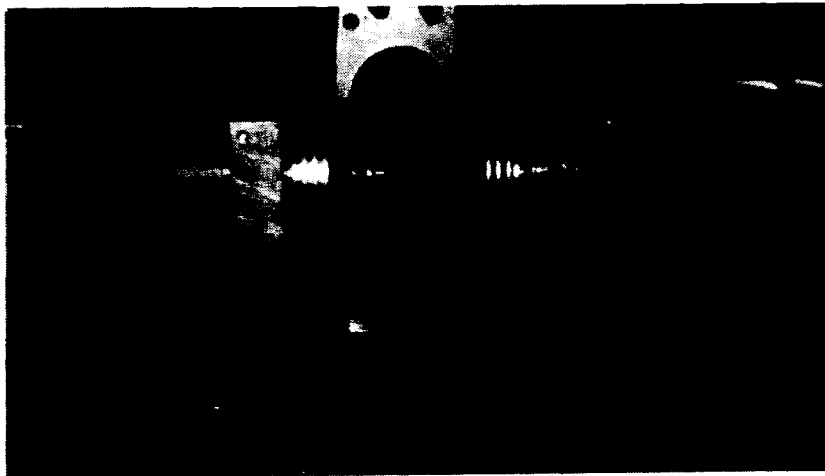


Fig. 1 - Steel specimen loaded on a rotating bending Schenck machine

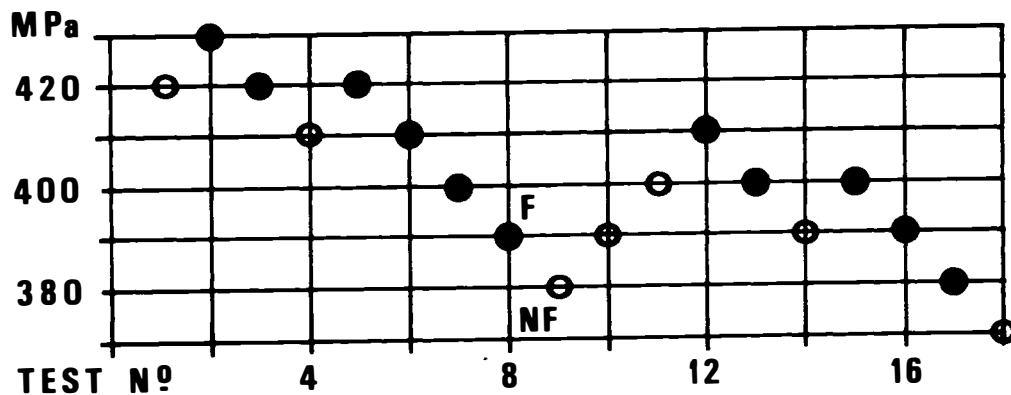


Fig. 2 - Standard method of determination of the endurance limit

4.4. Experimental results

Series of 5 rotating bending tests have been scanned by the infrared system at different stress levels. The load duration was chosen 60 seconds corresponding to 6 000 load cycles and 3 000 load cycles at 30 seconds in duration (Fig. 3). The software TIC 8000 allowed the data reduction : a subtraction of thermal images shows heat generation after 3,000 and 6,000 load cycles (Fig. 4).

The fatigue damage mechanism seems to be revealed by the change of intrinsic dissipation regime. Experimental results have been summarized in Fig. 5 where it can be seen how the endurance limit may be determined using a graphic procedure. The threshold of critical thermal dissipation is roughly the same for the 3,000 cycles and 6,000 cycles curves and it corresponds to the value deduced from standard procedure.

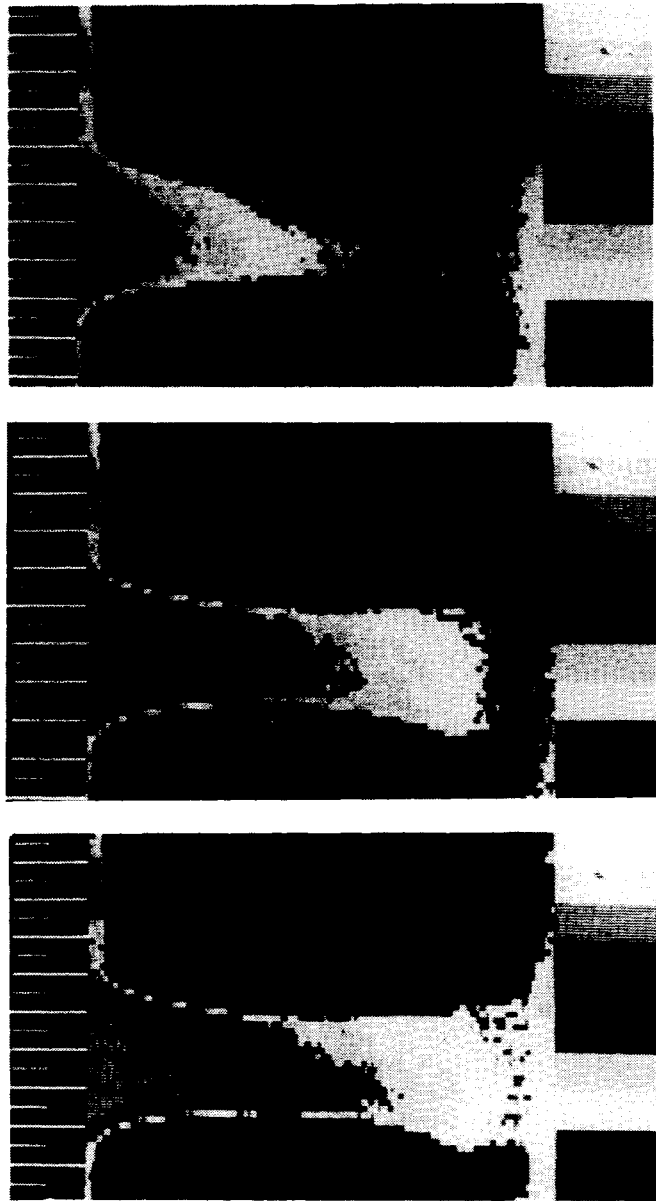
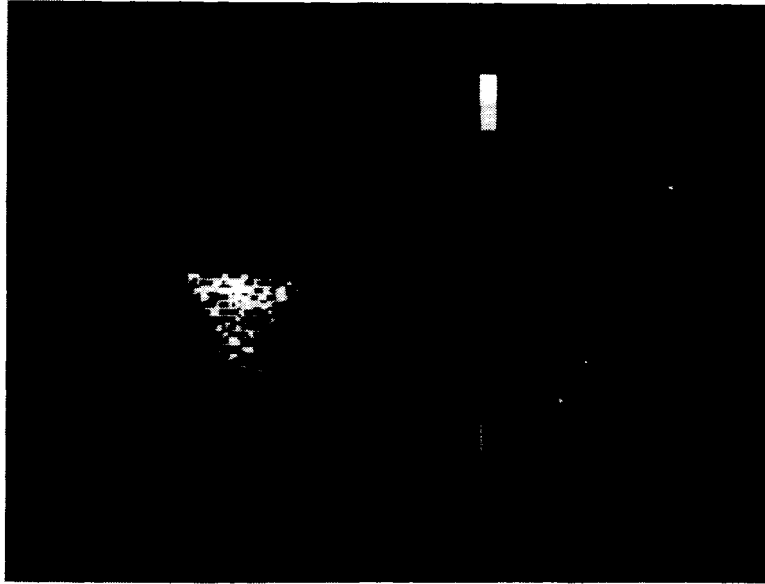
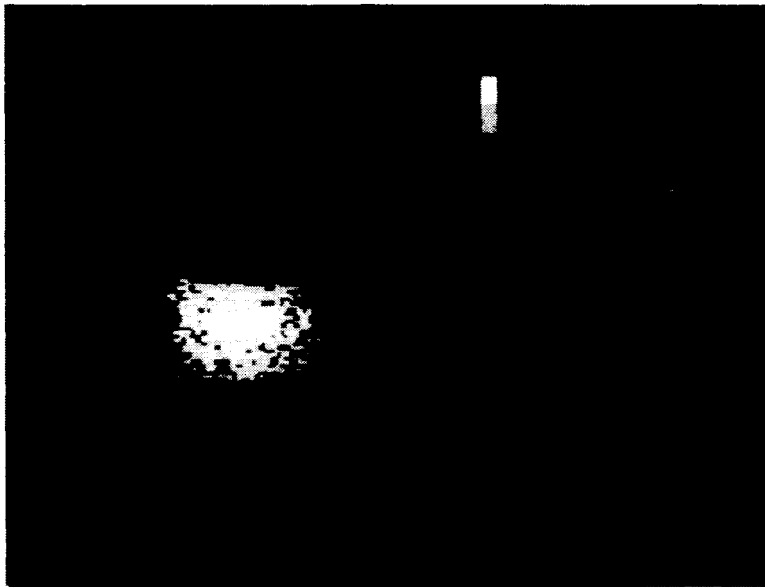


Fig. 3 - Thermograms of the specimen under 370 MPa and after 3,000 - 6,000 load cycles
(0.2 °C for each color hue)



Heat generation after 3,000 load cycles



Heat generation after 6,000 load cycles

Fig. 4 - Data reduction using TIC 8000 AGA software for a steel specimen subject to 370 MPa

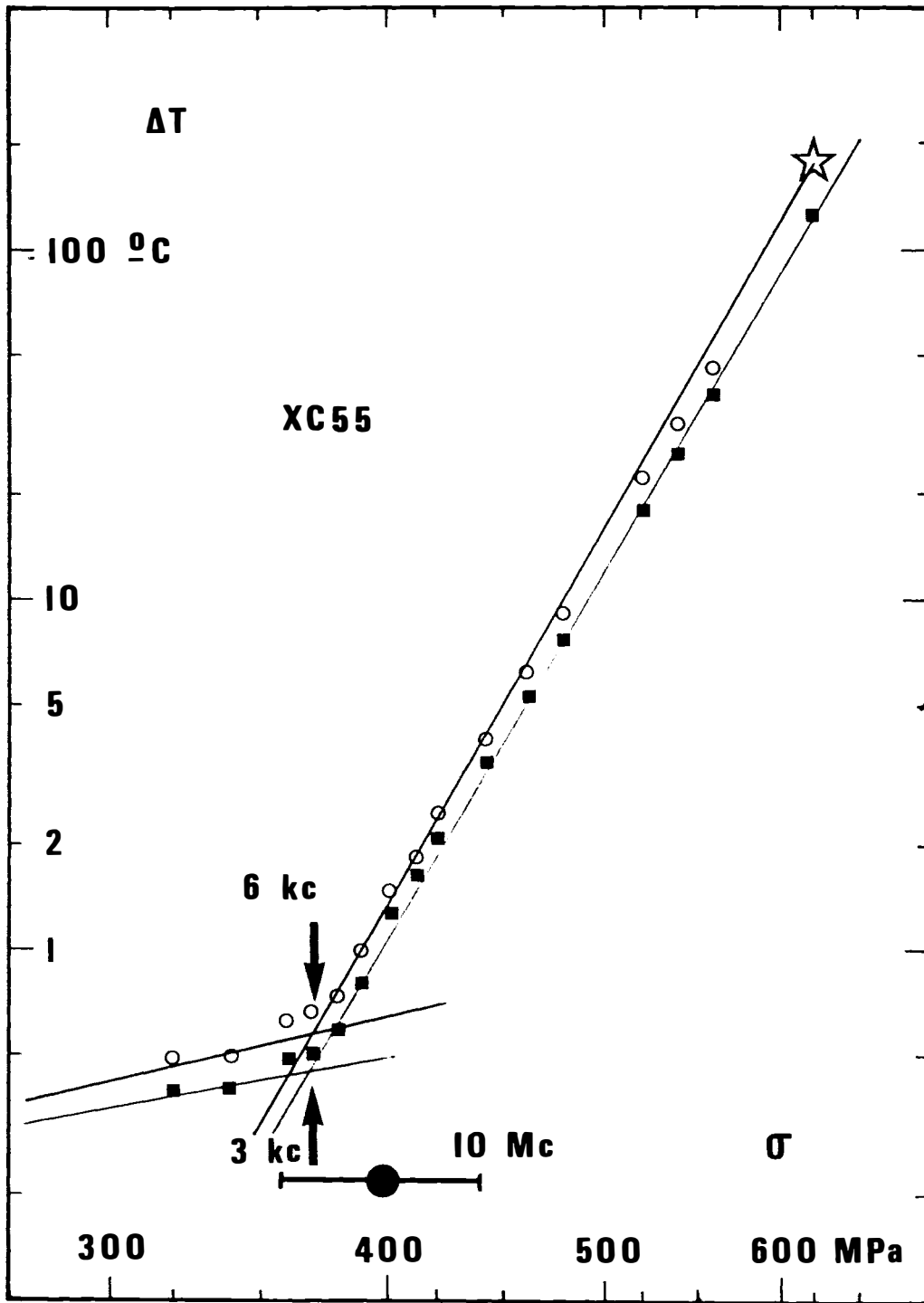


Fig. 5 - Graphic determination of the endurance limit

5. CONCLUDING REMARKS

Owing to the thermomechanical coupling, infrared thermography offers the possibility of a nondestructive, noncontact and in real time test to observe the physical process of metal degradation and to detect the occurrence of energy dissipation. Thus it readily allows a measure of the material damage and permits to evaluate the limit of a progressive damaging process under load beyond which the material is led to failure.

It is of particular interest that the method allows not only qualitative work such as finding flaws, but also quantitative analysis of the effects of flaws on strength and durability of structural components. This useful and promising technique allows accurate illustration of the initiation of a crack, the onset of its unstable propagation through the material and/or flaw coalescence when increasing irreversible microcracking is generated by vibratory loading. Particularly in case of fatigue testing, infrared thermography offers the possibility of a nondestructive, noncontact technique of damage detection, making evidence of the initiation of a crack and its propagation through the material. Detecting a strong change of intrinsic dissipation regime, this method readily allows an evaluation of the endurance limit, commonly determined by a very time-consuming procedure.

The main interest of this energy approach is to unify microscopic and macroscopic testing data. Subsequently it may suggest multiaxial design criteria, highly relevant for full scale testing on engineering structures.

6. REFERENCES

1. AGA Infrared Systems AB, "Thermovision 782", *Operating manual*, 1984.
2. D.H. Allen, "A prediction of heat generation in a thermoviscoplastic uniaxial bar", *Int. J. Solids Struct.*, 21, 4, 325-342, 1985.
3. H. Blok, *Applied Science Research A5*, 151, 1954.
4. H.D. Bui, A. Ehrlicher et Q.S. Nguyen, "Etude expérimentale de la dissipation dans la propagation de fissure par thermographie infrarouge", *C.R. Acad. Sci.*, 293, II, 1015-1017, 1981.
5. H.D. Bui and C. Stolz, "Damage theories for brittle and ductile materials", Herrmann and Larsson ed., *Fracture of Non-Metallic Materials*, 33-46, 1987.
6. J. Charrier et J.A. Marucic, "Possibilités d'utilisation des méthodes thermiques à des fins d'essais non destructifs en génie civil. Synthèse bibliographique", *Rap. de rech. LPC-MULT-LCPC*, 11, 1982.
7. O.W. Jr Dillon, "Coupled thermoplasticity", *J. Mech. Phys. Solids*, 11, 21-23, 1963.
8. C.E. Feltner and J.D. Morrow, "Microplastic strain hysteresis energy as a criterion for fatigue fracture", *ASME Journal of Basic Engineering*, 83, 15-22, March 1961.
9. A.M. Freudenthal and J.H. Weiner, "On the thermal aspect of fatigue", *Journal of Applied Physics*, 27, 1, 44-50, January 1956.
10. G. Gaussorgues, *La thermographie infrarouge*, Ed. *Technique et Documentation*, Lavoisier, Paris, 1984.
11. A.H.I. Gomma, "Corrélation entre la dissipation thermique d'une éprouvette en torsion alternée et sa limite d'endurance en fatigue", *Thèse Docteur-Ingénieur en Mécanique Physique*, Université de Bordeaux I, 1980.
12. G.R. Irwin, "Fracture", in *Encyclopedia of Physics II*, Springer Verlag, Heidelberg, 7, 1956.
13. J. Kratochvil and O.W. Dillon, "Thermodynamics of elastic-plastic materials as a theory with internal state variables", *J. Appl. Phys.*, 40, 3207-3218, 1969.
14. J. Kratochvil and O.W. Dillon, "Thermodynamics of crystalline elasticviscoplastic materials", *J. Appl. Phys.*, 11, 1470-1479, 1970.
15. E.H. Lee, "Elastic plastic deformations at finite strains", *J. Appl. Mech.*, 36, 1-6, 1969.
16. Th. Lehman, "Coupling phenomena in thermoplasticity", *5th Int. Conf. on Structural Mechanics in Reactor Technology*, Paper L1/1, Berlin, 1979.
17. M.P. Luong, *Infrared Vibrothermography of Plain Concrete*, Magnetic sound 16mm-film, Videotape UMATIC VHS PAL SECAM Systems ed. by IMAGICIEL, Ecole Polytechnique, 91128 Palaiseau, France, 1984.

18. M.P. Luong, "Characteristic threshold and infrared thermography of sand", *Geotechnical Testing J., GTJODJ*, 9, 80-86, 1986.
19. M.P. Luong, "Infrared observations of damage and fracture on concrete", *Thermomechanical Couplings in Solids*, ed. by H.D. Bui and Q.S. Nguyen, 85-94. Elsevier, Amsterdam, 1987.
20. J.D. Morrow, "Cyclic plastic strain energy and fatigue of metals", *Internal friction, damping and cyclic plasticity*, STP 378, ASTM, 45-84, July 1965.
21. Z. Mroz and B. Raniecki, "On the uniqueness problem in coupled thermoplasticity", *Int. J. Eng. Sci.*, 14, 211-221, 1976.
22. H.A. Nied and S.C. Batterman, "On the thermal feedback reduction of latent energy in the heat conduction equation", *Mater. Sci. Eng.*, 9, 243-245, 1972.
23. B. Raniecki and A.Sawczuk, "Thermal effects in plasticity", *Z. Angew. Math. Mech.*, 55, part 1, 333-341 and part 2, 363-373, 1975.
24. K.L. Reifsnider, E.G. Henneke and W.W. Stinchcomb, "The mechanics of vibrothermography", In *Mechanics of nondestructive testing* ed. by W.W. Stinchcomb, 249-276, 1980.
25. S.T. Rolfe and J.M. Barsom, *Fracture and fatigue control in structures - Applications of fracture mechanics*, Prentice-Hall, 1977.
26. G.I. Taylor and W.S. Farren, "The heat developed during plastic extension of metals", *Proc. Roy. Soc.*, 1, 107 : 422, 1925.
27. R. Tepfers, C. Friden and L. Georgsson, "A Study of the Applicability to the Fatigue of Concrete of the Palmgren-Miner Partial Damage Hypothesis", *Magazine of Concrete Research*, 29, 100, 123-130, 1977.
28. R. Tepfers, B. Hedberg and G. Szczekocki, "Absorption of Energy in Fatigue Loading of Plain Concrete", *Matériaux & Construction*, 17, 97 : 59-64, 1984.
29. C. Zener, *Elasticity and anelasticity of metals*, Chicago University Press, Chicago, 1948.